Chalcogenide Letters Vol. 11, No. 12, December 2014, p. 619 - 628

AB INITIO CALCULATION OF THE THERMODYNAMIC PROPERTIES OF WURTZITE ZnS: PERFORMANCE OF THE LDA AND GGA

Y. YU[*], D. FANG, G.D. ZHAO, X.L. ZHENG
College of Optoelectronic Technology, Chengdu University of Information Technology, Chengdu 610225, China

The thermodynamic properties of wurtzite ZnS are investigated by performing *ab initio* density functional theory and density functional perturbation theory calculations. Using both the local density approximation and generalized gradient approximation for the exchange-correlation potential, we calculate the phonon dispersion curves and the phonon density of states. The calculated phonon frequencies at the center zone for the Raman-active and infrared-active modes (including LO-TO splitting) are assigned. The thermodynamic functions are calculated by using the phonon density of states. The calculated values are in reasonable agreement with experimental data and other calculations.

(Received October 22, 2014; Accepted December 1, 2014)

Keywords: ZnS, DFPT, LO-TO splitting, Thermodynamic

1. Introduction

Zinc sulfide (ZnS) is found in nature mostly in the zinc-blende (zb) cubic structure and constitutes the standard ore for the smelting of zinc. It is also found as the mineral wurtzite (wz), which lends its name to the canonical 2H structure in which several tetrahedral semiconductors crystallize (e.g., CdS, CdSe, and GaN). As an important II-VI compound semiconductor, ZnS with a wide direct band gap has been extensively investigated and used in electroluminescent devices, infrared windows, flat panel displays, laser devices, sensors, etc [1, 2]. In spite of remarkable progress in the growth of ZnS and in the fabrication technologies of the devices using the material, some basic properties of ZnS, especially the lattice dynamics and thermodynamic properties study of wz ZnS, still remain poorly studied. The phonon spectrum is one of the fundamental characteristics of crystal. The behavior of phonon dispersion branches reflects specific features of the crystal structure and the interatomic interactions and, therefore, gives the most comprehensive and detailed information about the dynamical properties of crystals. The knowledge of various prominent features of phonon density of states (DOS) spectrum of solid is important for a general theoretical understanding and detailed quantitative description of its thermodynamic properties.

Several experiment and theory have been performed to study the dynamical and thermodynamical properties of wz ZnS. On the experimental side, Raman spectroscopy has been used to obtain the zone center phonon frequencies of wz ZnS [3-5]. However, identification of lattice modes in experimental studies is sometimes incomplete, partly because of the complexity of the structure and partly because of the experimental erroes. There are still some ambiguous assignments of the Raman modes for wz ZnS. To the best of our knowledge, despite of the interest in wz ZnS, the thermodynamic properties are at present poorly known. From a theoretical point of view, there have been only a few attempts to calculate the lattice dynamical and a detailed knowledge is still lacking. Cheng *et al*. [6] calculated the zone center frequencies using density

---

[*] Corresponding author: yuyoucuit@163.com

functional perturbation theory (DFPT) [6, 7]. Although the calculated phonon frequencies were found to be in good agreement with experimental results, the B_1 mode and Born effective charges were not reported. Hu *et al*. [8] only calculated the heat capacity C_V and Debye temperature Θ using density functional theory (DFT). Wang [9] only reported the anisotropic thermal expansion of wz ZnS using DFT and DFPT.

For *ab initio* calculations, the exact form of the exchange-correlation functional is not known, and one has to use various approximate schemes; the most widely used ones being the local density approximation (LDA) and generalized gradient approximation (GGA). It has been known that the LDA tends to "overbind", giving lattice constants that are too small and bulk moduli, phonon frequencies, and cohesive energies that are too large. The GGA seems to overcorrect these errors, giving lattice constants that are too large [10]. We are not aware of any detailed studies comparing the performance of the LDA and GGA in describing harmonic effects, which manifest themselves in the temperature dependence of the phonon contribution to the Helmholtz free energy ΔF, the phonon contribution to the internal energy ΔE, the entropy S, and the constant-volume specific heat C_V. In this paper, we have performed *ab initio* calculations to study the thermodynamic properties of wz ZnS, using both the LDA and GGA.

2. Computational details

All of the results reported in this paper were obtained by using ABINIT [11] implementation of the DFT and DFPT with a plane-wave basis set for the electronic wave functions and periodic boundary conditions. The exchange correlation potential was considered by the LDA with the form of Ceperley-Adler parameterized by Perdew and Zunger [12] and GGA with the correction of Perdew-Burke-Ernzerhof version [13], respectively. The wave functions are expanded in plane waves up to a kinetic energy cutoff of 40 hartree. Integrals over the Brillouin zone (BZ) are replaced by a sum on a Monkhorst-pack grid of 4×4×4 special **k-**point. Convergence tests show that the BZ sampling and the kinetic energy cutoff are sufficient to guarantee an excellent convergence.

The structural parameters are obtained by optimizing lattice constants and atomic coordinates until all force components are below 1×10^{-6} Hartree/Bohr. After geometry optimizations, the relaxed structures are used in lattice dynamics and thermodynamics calculations. The correct temperature variation of the thermodynamic properties can be obtained by treating the lattice vibrations as quantized (phonons) [14, 15].

3. Results and discussion

3.1 Structural properties

The wz ZnS compound has wurtzite structure (space group $P6_3mc$) with two Zn and two S atoms per unit cell. At first, we have optimized the structure parameters using the experimental parameters ($a = b = 3.811$ Å, $c = 6.234$ Å, and $u = 0.375$, respectively) [16] to construct an initial unit cell. The lattice parameters are determined from atomic and structural relaxation. It is well known that LDA often underestimates the equilibrium lattice constant, whereas the GGA has a tendency to overcorrect the LDA error and results in overestimations. To judge about the accuracy of our calculations, we have compared LDA and GGA calculations with available experimental data. The calculated lattice parameters, a, c, c/a, V and u, are compared to other calculations and experimental data reported in the literature in Table 1. It is found that the calculated lattice constants for LDA calculation agree well with experimental ones with the errors not exceeding 2%, and the errors of GGA are 2% higher than relative values. As expected, the experimental values for the lattice constants lie sandwiched between the LDA and GGA values. This is largely sufficient to allow the further study of vibrational and thermodynamic properties.

Table 1. Calculated lattice parameters compared with reported experimental and theoretical values.

Method	a_0	c_0	u
ABINIT-LDA (This work)	3.763	6.156	0.3745
ABINIT-GGA (This work)	3.885	6.345	0.3744
QUANTUMN-ESSPRESSO-GGA (Ref. [5])	3.810	6.248	
FP-LAPW-LDA (Ref. [17])	3.760	6.140	0.374
CRYSTAL98-HF (Ref. [18])	3.982	6.500	0.377
Exp. (Ref. [16])	3.811	6.234	0.375
Exp. (Ref. [19])	3.8227	6.2607	0.3748

3.2 Dielectric properties

Both the dielectric tensor $\varepsilon(\infty)$ and Born effective charge tensor $Z^B(\kappa)$ are required to understand the influence of the macroscopic electric field on lattice dynamics properties. The objective of our work is to employ the study of the dielectric tensors and Born effective charge tensors, to obtain the lattice dynamics of the wz ZnS. The macroscopic dielectric tensor $\varepsilon(\infty)$ is formally defined as

$$\varepsilon_{\alpha\beta}(\infty) = 1 + 4\pi \frac{\partial P_\alpha}{\partial E_\beta}, \tag{1}$$

where ***P*** is the macroscopic electronic polarization induced by the screened electric field ***E***. On the other hand, the tensor of Born effective charges

$$Z^B_{\alpha\beta}(\kappa) = \frac{V}{e}\frac{\partial P_\alpha}{\partial u_\beta(\kappa)} \tag{2}$$

is a measure of the polarization induced by a displacement ***u*** of the κth atom at vanishing electric field. Table 2 shows the results for the dielectric tensor $\varepsilon(\infty)$ and Born effective charges tensor Z^B of wz ZnS using both the LDA and GGA, compared to the theoretical [20] and experimental data [21]. For the wurtzite structure $\varepsilon(\infty)$ is composed of two independent components, one corresponding to the direction parallel to the *c* axis, $\varepsilon_\parallel(\infty) = \varepsilon_{zz}(\infty)$, and the other being characteristic for the hexagonal plane perpendicular to the *c* axis, $\varepsilon_\perp(\infty) = \varepsilon_{xx}(\infty) = \varepsilon_{yy}(\infty)$. The average dielectric tensor $\varepsilon(\infty) = 1/3Tr\varepsilon(\infty)$ is also included in Table 2. Form comparison, Wright *et al.* [20] obtained the dielectric tensor using new interatomic potentials method. $\varepsilon(\infty)$ from Ref. [20] is 4.83 and the corresponding experimental value is 5.7 [21], while our calculated values are 7.81 for LDA and 7.30 for GGA. It can be seen that both LDA and GGA overestimate the dielectric tensors. Discrepancies can be attributed to well-known LDA and GGA underestimation of the band gap as well as the fact that our calculation represents 0 K, while the experiment was done at room temperature. Dielectric tensors are also somewhat dependent (at the ~ 5% level) on the choice of pseudopotential.

Table 2. The components of the dielectric tensor $\varepsilon(\infty)$ *and Born effective charge* Z^B *of wz ZnS, perpendicular* ($\perp$) *and parallel* (||) *to the c axis, and their average values.*

	$\varepsilon_\perp(\infty)$	$\varepsilon_\parallel(\infty)$	$\varepsilon(\infty)$	$Z_\perp^B$	$Z_\parallel^B$	Z^B
LDA (This work)	7.81	6.29	7.30	2.17	1.97	2.10
GGA (This work)	7.30	5.99	6.86	2.27	2.11	2.22
Theor. (Ref. [20])	4.79	4.91	4.83	1.41	1.34	1.39
Exp. (Ref. [21])			5.7			

The Born effective charge $Z^B(\kappa)$ represents the charge of the κth ion interacting with the macroscopic electric field. $Z^B(\kappa)$ is also referred to as dynamic effective charge as distinct from the static effective that results from the static transfer of the electron charge density from the cation to the anion when a crystal is formed [22]. The translational invariance of the crystal (the charge neutrality condition) imposes an important relationship between the components of the tensor of the Born effective charges that is known as the acoustic sum rule (ASR) [23]. For the zinc-blende structure, the tensor of Born effective charges is isotropic. Because of the charge neutrality the charges of the cation and anion only differ by the sign. In the wurtzite case the tensor components parallel and perpendicular to the *c* axis are independent of each other. Although there are four atoms in the unit cell, the nonsymmorphic space group C_{6v}^4 with a screw axis along the *c* axis enforces that only two of them are independent [24]. Furthermore, because of the charge neutrality condition we have to consider only one tensor of Born effective charges with two independent components $Z_\perp^B = Z_{xx}^B = Z_{yy}^B$ and $Z_\parallel^B = Z_{zz}^B$. It is seen that the difference between the LDA and GGA results is small. To the best of our knowledge, no experiment data of the Born effective charges for wz ZnS exist. It has been already noticed by Wright *et al.* that the values of the Born effective charges vary around 1.39 [20] and the tensors are similar in form to ours. The difference between our results and those of Ref. [20] might be due to the use of different types of interatomic potentials.

3.3 Vibrational properties

ZnS with the wurtzite structure belongs to the point group C_{6v} (6 mm) and space group $P6_3mc$ with two formula units per primitive cell. A crystal lattice with *n* atoms per unit cell has 3*n* branches, three of which are acoustic and the remainder optical. There are 4 atoms in the primitive unit cell of wz ZnS crystal, so there are 12 dispersion curves, which mean 12 normal vibration modes at the center Γ point. The irreducible representations of the lattice vibration in wz ZnS are the following: $\Gamma = \Gamma_{aco} + \Gamma_{opt} = 2A_1 + 2B_1 + 2E_1 + 2E_2$, of which one A_1 and one E_1 are both Raman active and infrared active; the two E_2 are only Raman active; and the B_1 modes are silent. Due to the macroscopic electric field associated with the atomic displacements of the longitudinal optical phonons, the A_1 and E_1 optical modes are each split into LO and TO components.

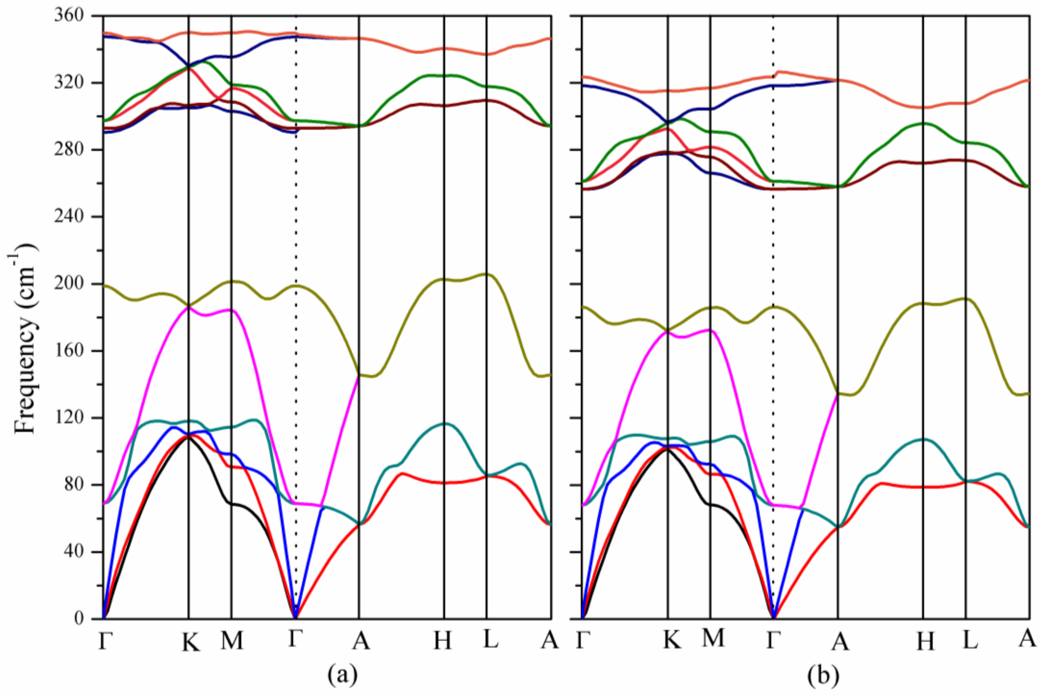

Fig. 1. Calculated phonon dispersion curves along symmetry lines in the Brillouin zone for wz ZnS using the (a) LDA and (b) GGA.

The results for the phonon dispersion curves of wz ZnS are displayed in Fig. 1 along several high-symmetry lines and the corresponding phonon DOS are shown in Fig. 2, calculated using the DFPT with the LDA and GGA. The phonon DOS is normalized to the number of phonons. Our calculations show that the spectra of the crystal consist of two bands and have the limit at about 350 cm^{-1} for the LDA and 330 cm^{-1} for the GGA. One finds that a clear gap opens between the six upper energy branches and the remaining six dispersion branches. The LDA and GGA frequency gaps are about 90 cm^{-1} and 70 cm^{-1}, respectively. Despite the similarity, there are also several distinctions in the phonon DOS due to the different phonon frequencies.

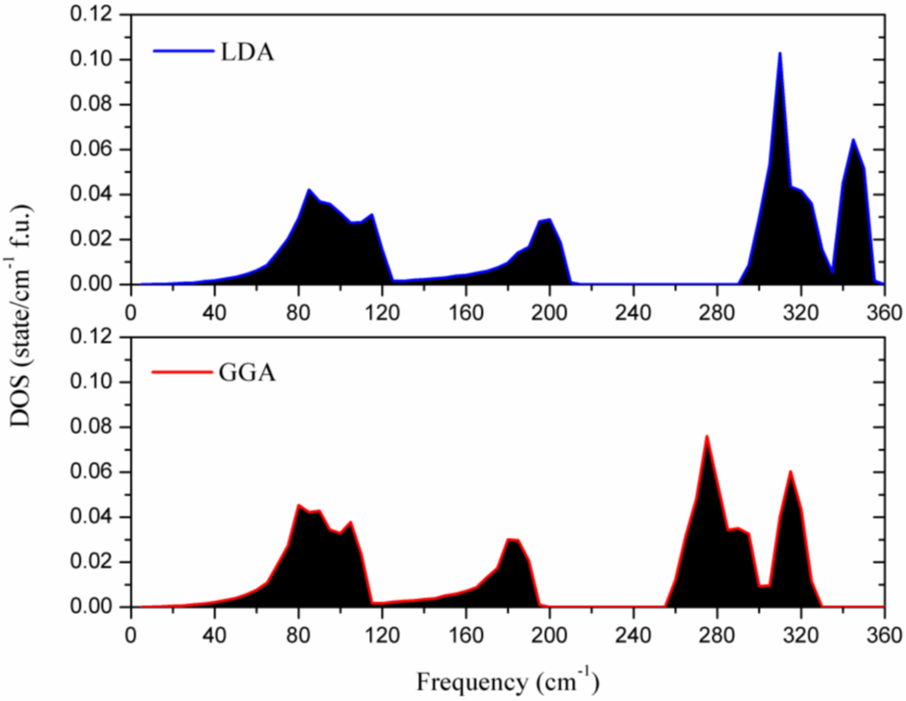

Fig. 2. Phonon density of state for wz ZnS using the LDA and GGA.

The results for the zone-center (Γ points) phonon frequencies and their symmetry assignments are displayed and compared with the experimental values [3-5] and other calculations [5] in Table 3. It is seen that the agreement with experiment is quite good, though the LDA overestimates phonon frequencies and the GGA underestimates them, which is consistent with previous reports [10]. The overestimation (underestimation) of the frequencies by the LDA (GGA) can be traced back to the underestimation (overestimation) of the lattice constant. The measured frequencies of A_1(LO) and E_1(TO) modes are too close to be distinguished that they are both assigned the same value [3, 5]. The calculated frequencies of the two modes are at 350 and 349 cm^{-1} for the LDA (327 cm^{-1} and 324 cm^{-1} for the GGA), which have a discrepancy of only 1 cm^{-1} (3 cm^{-1} for the GGA). From previous experimental studies, B_1 was not observed. In addition, the phonon frequencies of wz ZnS were calculated by Cheng *et al.* [5] but B_1 mode was not reported. However, B_1 modes predicted by group theory were assigned in present work for the first time.

Table 3. Phonon frequencies (unit: cm^{-1}) at zone-center (Γ point) of wz ZnS.

Symmetry	This work		Exp. (Ref. [4])		Exp. (Ref. [3])	Exp. (Ref. [5])	Theor. (Ref. [5])
	LDA	GGA	300 K	140 K			
E_2(low)	69	68	69.2	69.4	72		76
B_1(low)	199	186					
A_1(TO)	290	257	267	272	273	275	287
E_1(TO)	293	257	273	276	273	279	288
E_2(high)	297	261	283	286	286	285	296
B_1(high)	347	318					
A_1(LO)	350	327			351	353	350
E_1(LO)	349	324	347.8	350.5	351	353	347

3.4 Thermodynamic properties

The knowledge of the entire phonon spectrum granted by DFPT makes possible the calculation of several important thermodynamical properties as functions of temperature T. In the present work, the phonon contribution to the Helmholtz free energy ΔF, the phonon contribution to the internal energy ΔE, the entropy S, and the constant-volume specific heat C_V, at temperature T, are calculated using the formulas in Ref. 25 within the harmonic approximation:

$$\Delta F = 3nNk_B T\int_0^{\omega_{\max}} \ln\left\{2\sinh\frac{\hbar\omega}{2k_B T}\right\} g(\omega)d\omega , \tag{3}$$

$$\Delta E = 3nN\frac{\hbar}{2}\int_0^{\omega_{\max}} \omega\coth\left(\frac{\hbar\omega}{2k_B T}\right) g(\omega)d\omega , \tag{4}$$

$$S = 3nNk_B\int_0^{\omega_{\max}} \left[\frac{\hbar\omega}{2k_B T}\coth\frac{\hbar\omega}{2k_B T} - \ln\left\{2\sinh\frac{\hbar\omega}{2k_B T}\right\}\right]\times g(\omega)d\omega , \tag{5}$$

$$C_V = 3nNk_B \int_0^{\omega_{\max}} \left(\frac{\hbar\omega}{2k_BT}\right)^2 \operatorname{csch}^2\left(\frac{\hbar\omega}{2k_BT}\right) g(\omega)d\omega, \tag{6}$$

where k_B is the Boltzman constant.

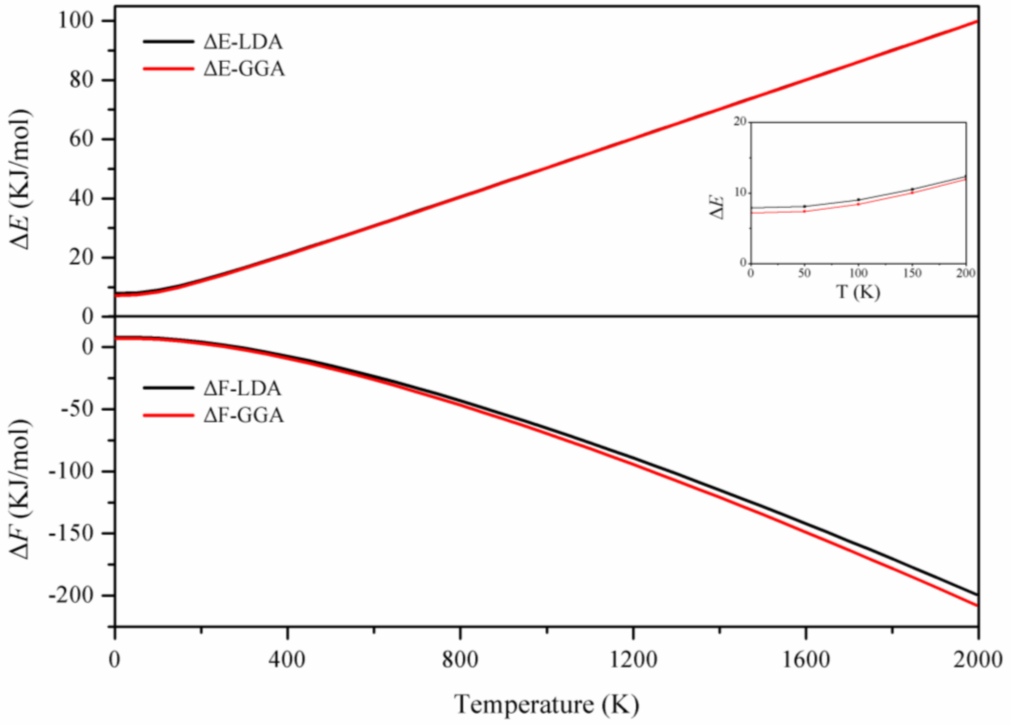

Fig. 3. Temperature dependence of ΔE and ΔF for wz ZnS using the LDA and GGA.

The Δ*F* and Δ*E* are shown in Fig. 3. Δ*F* and Δ*E* represent the zero-point motion at zero temperature, which can be calculated from the expression as $\Delta F_0 = \Delta E_0 = 3nN\int_0^{\omega_{\max}} (\hbar\omega/2)g(\omega)d\omega$, where *n* is the number of atoms per unit cell, *N* is the number of unit cells, ω is the phonon frequencies, $\omega_{\max}$ is the largest phonon frequency, and $g(\omega)$ is the normalized phonon DOS with $\int_0^{\omega_{\max}} g(\omega)d\omega = 1$. For wz ZnS, the calculated ΔF_0 (or ΔE_0) values are 7.88 kJ/mol and 7.16 kJ/mol for GGA and LDA, respectively. When the temperature increases, the discrepancy of Δ*E* between the LDA and GGA results is very small. It is noticed that Δ*F* decreases with the increment of temperature. The discrepancy of Δ*F* between the LDA and GGA results is small at low temperatures, but the LDA values are larger when the temperature is higher than 600 K. From Fig. 4, it can be seen that the GGA values of the entropy *S* lie in between the LDA and experimental values and for both the LDA and GGA the agreement with experiment [26] is excellent. The experimental values are slightly larger than the calculated values since the effects of anharmonicity are ignored and the theoretical lattice constants are used in the calculation.

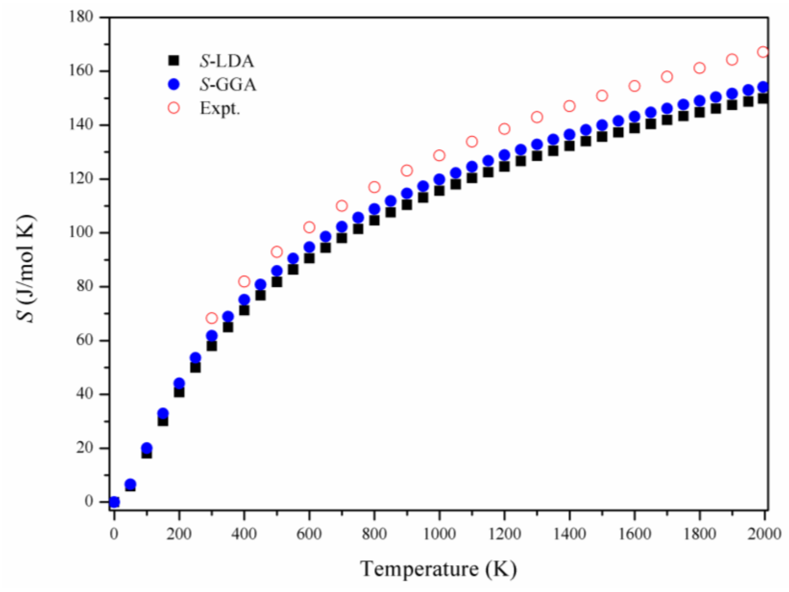

Fig. 4. Temperature dependence of S for wz ZnS using the LDA and GGA.

Fig. 5 shows the constant-volume specific heat C_V calculatd using Eq. (6) and compared to the experimentally available data for the constant-pressure specific heat C_P [26] and other similar theoretical calculation [8]. The agreement between both LDA and GGA calculations and experimental data is very good at room temperature. Below 250 K GGA results are slightly higher than LDA results and both exhibit the expected T^3 power-law behavior in the low-temperature limit. At high temperature LDA and GGA give almost identical C_V. The high temperature C_V does not reach a classical limit of 50 J/mol K up to 1000 K which is below the melting point of wz ZnS. The discrepancies between the calculated harmonic specific heat C_V and the experiment specific heat C_P above 300 K are indicative of vibrational anharmonicity.

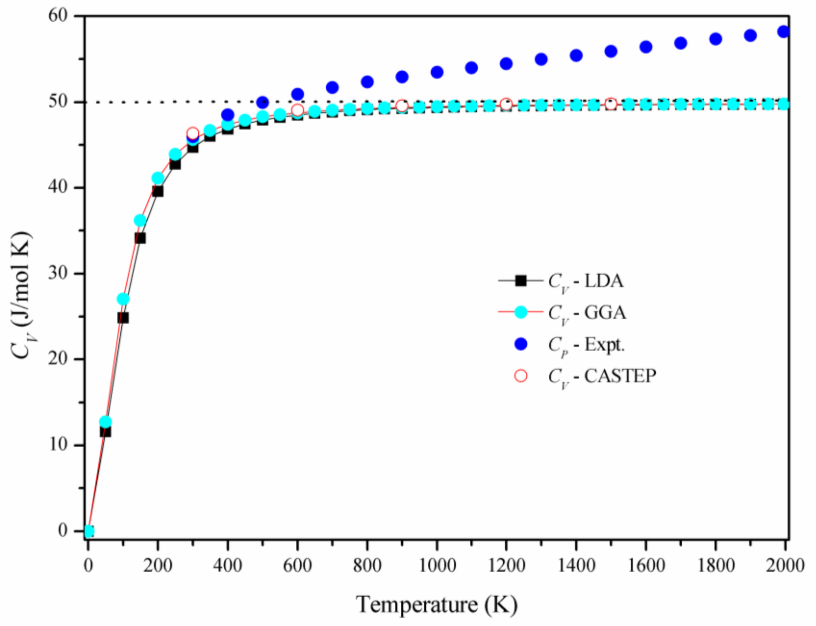

Fig. 5. Temperature dependence of C_V for wz ZnS using the LDA and GGA.

4. Conclusions

In summary, we have performed *ab initio* calculations to study the thermodynamical properties of wz ZnS, using phonon frequencies computed using DFPT. We have calculated the lattice parameters, the dielectric tensor $\varepsilon(\infty)$, the Born effective charge tensor Z^B, the phonon dispersion curves, the phonon contribution to the Helmholtz free energy ΔF, the phonon contribution to the internal energy ΔE, the entropy S, and the constant-volume specific heat C_V. All of the above have been computed using both the LDA and GGA.

In this work, we have found that structural and vibrational properties depend significantly on the choice of exchange-correlation functionals (LDA versus GGA). LDA systematically underestimates the lattice constant and the Born effective charge tensor Z^B, whereas the GGA overestimates these. In contrast, the LDA always overestimates the dielectric tensor $\varepsilon(\infty)$ and phonon frequencies, and the GGA underestimates them. All vibrational modes are identified and compared with experiments and previous theoretical calculations. The calculated zone-center phonon mode frequencies are in good agreement with Raman experiments. The thermodynamics properties including the phonon contribution to the Helmholtz free energy ΔF, the phonon contribution to the internal energy ΔE, the entropy S, and the constant-volume specific heat $C_V$are determined within the harmonic approximation based on the calculated phonon dispersion relations. The thermodynamics properties are also affected by the choice of exchange-correlation functional. We believe that these theoretical predictions should be highly valuable for the experimental community in framework of the characterization of wz ZnS.

References

[1] G.Z. Shen, Y. Bando, J.Q. Hu, D. Golberg. Appl. Phys. Lett. **90,** 123101 (2007).
[2] T. Yamamoto, S. Kishimoto, S. Iida. Phys. Rev. B **308-310,** 916 (2001).
[3] O. Brafman, S.S. Mitra, Phys. Rev. **171,** 931 (1968).
[4] J. Schneider, R.D. Kirby, Phys. Rev. B **6,** 1290 (1972).
[5] Y.C. Cheng, C.Q. Jin, F. Gao, X.L. Wu, W. Zhong, S.H. Li, Paul K. Chu, J. Appl. Phys. **106,** 123505 (2009).
[6] S. Baroni, P. Giannozzi, A. Testa, Phys. Rev. Lett. **58,** 1861 (1987).
[7] S. Baroni, S. de Gironcoli, A. Dal Corso, P. Giannozzi, Rev. Mod. Phys. **73,** 515 (2001).
[8] C.E. Hu, Z.Y. Zeng, Y. Cheng, X.R. Chen, L.C. Cai, Chin. Phys. B **17,** 3867 (2008).
[9] S.Q. Wang, Appl. Phys. Lett. **88,** 061902 (2006).
[10] S. Narasimhan, S. de Gironcoli, Phys. Rev. B **65,** 064302 (2002).
[11] X. Gonze, J.-M. Beuken, R. Caracas, F. Detraux, M. Fuchs, G.-M. Rignanese, L. Sindic, M. Verstraete, G. Zerah, F. Jollet, M. Torrent, A. Roy, M. Mikami, Ph. Ghosez, J.-Y. Raty, D.C. Allan, Comput. Mater. Sci. **25** (2002) 478. http://www.abinit.org.
[12] J.P. Perdew and A. Zunger, Phys. Rev. B **23,** 5048 (1981).
[13] J.P. Perdew, S. Burke and M. Ernzerhof, Phys. Rev. Lett. **77,** 3865 (1996).
[14] A. Kellou, T. Grosdidier, C. Coddet, H. Aourag, Acta Mater. **53,** 1459 (2005).
[15] A.A. Maradudin, E.W. Montroll, C.H. Weiss, I.P. Ipatova, *Theory of Lattice Dynamics in Harmonic Approximation*, 2nd ed. (Academic, New York, 1971), Chap. 4.
[16] Y.-N. Xu, W.Y. Ching, Phys. Rev. B **48,** 4335 (1993).
[17] H. Rozale, L. Beldi, B. Bouhafs, P. Ruterana, phys. Stat. Sol. (b) **244,** 1560 (2007).
[18] M. Catti, Y. Noel, R. Dovesi, J. Phys. Chem. Solids **64,** 2183 (2003).
[19] E.H. Kisi, M.M. Elcombe, Acta Crystallogra **C45**, 1867 (1989).
[20] K. Wright, Julian D. Gale, Phys. Rev. B **70,** 035211 (2004).

[21] Landolt-Bornstein, *New Series III* (Springer, Berlin, 1987), Vol. 22.
[22] W.A. Harrison, *Electronic Structure and Properties of Solids* (Dover, New York, 1989).
[23] R. Pick, M.H. Cohen, R.M. Martin, Phys. Rev. B **1,** 910 (1970).
[24] K. Karch, J.-M. Wagner, F. Bechstedt, Phys. Rev. B **57,** 7043 (1998).
[25] C. Lee and X. Gonze, Phys. Rev. B **51,** 8610 (1995).
[26] I. Barin, *Thermochemical Data of Pure Substances*, 3rd ed. VCH, New York, 1995.